Neuropilin-1 aggravates liver cirrhosis by promoting angiogenesis via VEGFR2-dependent PI3K/Akt pathway in hepatic sinusoidal endothelial cells

Le Wang [a,b,1], Yuemin Feng [a,b,1], Xiaoyu Xie [a,b], Hao Wu [a,b], Xiao Nan Su [a,b], Jianni Qi [b,c], Wei Xin [c], Lifen Gao [d], Ying Zhang [e], Vijay H. Shah [f], Qiang Zhu [a,b,*]

[a] Department of Gastroenterology, Shandong Provincial Hospital Affiliated to Shandong University, Jinan, Shandong, China
[b] Shandong Provincial Engineering and Technological Research Center for Liver Diseases Prevention and Control, Jinan, Shandong Province, China
[c] Department of Central Laboratory, Shandong Provincial Hospital Affiliated to Shandong University, Jinan, Shandong Province, China
[d] Key Laboratory for Experimental Teratology of Ministry of Education, Key Laboratory of Infection and Immunity of Shandong Province, Department of Immunology School of Basic Medicine, Shandong University, Jinan, Shandong Province, China
[e] Department of Molecular Microbiology and Immunology, Bloomberg School of Public Health, Johns Hopkins University, Baltimore, MD 21205, USA
[f] Gastroenterology Research Unit, Mayo Clinic and Foundation, Rochester, MN, USA

ARTICLE INFO

ABSTRACT

Background: We have revealed that neuropilin-1 (NRP-1) promoted hepatic stellate cell activation and liver fibrosis through its profibrogenic signalling pathways. However, the role of NRP-1 in angiogenesis in hepatic sinusoidal endothelial cells (HSECs) during liver cirrhosis remains unclear.

Methods: The correlation between NRP-1 expression and angiogenesis was evaluated in both human and murine cirrhotic liver tissues by immunohistochemical staining, quantitative real-time PCR, and western blotting. In addition, the role and mechanism of NRP-1 in regulating VEGFR2-dependent angiogenesis was identified in endothelial cells (ECs) in vitro. Moreover, liver histocultures were used to test the therapeutic effect of NRP-1 blocking in liver fibrosis.

Findings: Higher expression of NRP-1 in HSECs was detected, which was positively correlated with angiogenesis in liver cirrhosis. In vitro, NRP-1 knockdown suppressed the expression and activation of VEGFR2, accompanied by reduced ability of the vascular tube formation and the migration of ECs. Conversely, NRP-1 overexpression up-regulated VEGFR2, promoted tube formation, and the migration of ECs. Mechanistically, NRP-1 modulated the expression of VEGFR2 by regulating FAK and its kinase activity. Furthermore, NRP-1 promoted VEGFR2-dependent angiogenesis via the PI3K/Akt pathway in HSECs. Blocking NRP-1 function reduced intrahepatic angiogenesis and fibrosis-associated factors in the in vitro liver histocultures.

Interpretation: NRP-1 promotes angiogenesis by upregulating the expression and activation of VEGFR2 through the PI3K/Akt signalling pathway in liver cirrhosis. This study highlights the possibility of therapeutically targeting NRP-1 for the treatment of cirrhosis.

Fund: National Natural Science Foundation of China (No. 81570551; 81770607; 81600469; 81401868), Key Research project of Shandong Province (No. 2016GSF201008; 2017GSF218053), Natural Science Foundation of Shandong Province (No. ZR2017MH102), National Science and Technology Major Project of China (No. 2018ZX10302206-001-006).

1. Introduction

Liver cirrhosis, which develops from liver fibrosis, is one of the most severe pathological stages of all chronic liver injuries and can lead to severe clinical complications [1]. Liver cirrhosis is characterized by the deposition of extracellular matrix proteins and increased intrahepatic angiogenesis induced by the independent activation of hepatic stellate cells (HSCs) and hepatic sinusoidal endothelial cells (HSECs) [2]. HSECs represent the highest proportion of non-parenchymal cells in the liver and are also major co-modulators of fibrogenesis in addition to HSCs [3].

Research in context

Evidence before this study

Liver cirrhosis is characterized by excessive extracellular matrix deposition and increased intrahepatic angiogenesis induced by the independent activation of hepatic stellate cells and hepatic sinusoidal endothelial cells. Our previous study revealed that NRP-1 promoted hepatic stellate cell activation and liver fibrosis through its profibrogenic PDGF/TGF-β signalling pathway. However, the pro-angiogenetic role of NRP-1 in hepatic sinusoidal endothelial cells during liver cirrhosis remains unclear.

Added value of this study

We demonstrated that NRP-1 promoted intrahepatic angiogenesis by upregulating the expression and activation of VEGFR2 through the PI3K/Akt signalling pathway in liver cirrhosis. Of note, blocking NRP-1 function suppressed neoangiogenesis in HSECs and reduced intrahepatic angiogenesis and fibrosis-associated factors in the in vitro liver histocultures.

Implications of all the available evidence

The current study highlights the possibility of therapeutically targeting NRP-1 for the treatment of cirrhosis.

It is well known that vascular growth factors (VEGFs) play an important role in the regulation of angiogenesis via the receptors VEGFRs and NRPs [4]. NRP-1, which is the first member of the NRP group, was originally described as a class III semaphoring binding protein (SEMA3), which regulates axon guidance [5]. NRP-1 interacts with VEGFs to enhance cell angiogenesis and has been implicated in embryonic and tumour angiogenesis [6,7]. Targeting and blocking NRP-1 by various methods has been found to decrease tumour angiogenesis [8,9]. Our previous results have indicated that NRP-1 promoted liver cirrhosis progression, serving as a co-receptor of platelet-derived growth factor-B (PDGF-B) and transforming growth factor-β (TGF-β) [10]. Recent evidence has also indicated increased levels of angiogenesis and VEGFR2 expression in cirrhotic patients, suggesting they may play potential roles in the progression of liver cirrhosis [11,12]. Nevertheless, the role of NRP-1 in intrahepatic angiogenesis in HSECs remains unclear and requires further research.

NRP-1 is a multifaceted transmembrane receptor that binds VEGF as well as VEGFR2. Currently, it is widely accepted that NRP-1 promotes angiogenesis through VEGF-NRP-1 interaction, which further enhances VEGFR2 activity and downstream signalling [13,14]. However, other studies suggest that NRP-1 may also act independently of binding VEGF and may even modulate VEGFR2 activity in stimulating cell migration and adhesion to promote angiogenesis [15,16]. In addition, VEGFR2 activation initiates multiple intracellular signal transduction pathways involving p38, extracellular regulated protein kinases1/2(ERK1/2), phosphatidylinositol 3′-kinase(PI3K)/Akt, and Src/focal adhesion kinase (FAK) [17,18]. The mechanisms and signalling pathways of NRP-1 in HSECs-induced intrahepatic angiogenesis during liver cirrhosis progression remain largely unknown.

In the present study, we first show that the expression of NRP-1 significantly increased in HSECs during cirrhosis and was positively correlated with VEGFR2 and intrahepatic angiogenesis levels in vivo. Furthermore, we found that NRP-1 upregulated the expression and activation of VEGFR2 on a transcriptional level via FAK activity in HSECs, subsequently promoting intrahepatic angiogenesis through the PI3K/Akt signal pathway during cirrhosis progression. Meanwhile, liver

histoculture indicated that NRP-1 inhibition suppressed angiogenesis and fibrosis-associated factors. Collectively, our results revealed, for the first time, that NRP-1 aggravated cirrhosis by promoting HSECs-induced angiogenesis. Our data suggest that blocking NRP-1 might be a valuable therapeutic target to combat angiogenesis and fibrosis during cirrhosis.

2. Materials and methods

2.1. Human subjects

Seven cirrhotic liver tissues were obtained from surgical waste or biopsies for this study. Liver cirrhosis was diagnosed by histology or via clinical or imaging indicators. Three normal liver tissues from the surgical waste of liver traumas were collected from beyond the border of the abnormality and included as the control. No statistical difference in age or sex was observed between the cirrhotic or normal groups. Demographic and laboratory characteristics of the two groups are shown in Supplement Table 1. The liver tissues were collected for quantitative real-time PCR (qRT-PCR), western blotting, immunohistochemistry, and histological analysis. The authors obtained informed consent from each participant to conduct this study. All procedures were approved by the Ethics Committee of Shandong Provincial Hospital Affiliated to Shandong University (Jinan, China).

2.2. Cirrhotic animal models

C57BL/6 mice were purchased from Shandong University Laboratory Animal Centre and were administered CCl_4 (5 ml/kg, CCl_4, olive oil = 1:3) or olive oil twice a week by intraperitoneal injection over the course of 6 or 8 weeks. Mouse livers were harvested to examine for the expression of angiogenesis or fibrosis markers using western blotting, immunohistochemistry, and histological analysis. The animal study protocol was approved by the Ethics Committee of Shandong Provincial Hospital.

2.3. Cell culture and infection

Human HSECs (ScienCell, Carlsbad, CA, USA) were cultured in ECM with 10% foetal bovine serum (FBS), 1% penicillin/streptomycin, and 10% endothelial cell growth supplement (ScienCell). Human umbilical vein endothelial cells (HUVECs) purchased from the American Type Culture Collection (ATCC, Rockville, MD, USA) were cultured in Hams F12k medium with 10% FBS and 1% penicillin/streptomycin. SK-HEP-1 cells (Procell, Wuhan, CN) were cultured in MEM with 10% FBS and 1% penicillin/streptomycin.

Lentiviral transduction tagged with GFP to downregulate or overexpress NRP-1 was performed in HSECs, HUVECs, and SK-Hep-1 cells according to the instructions from the manufacturer using 20 MOI of lentivirus-encoding target genes. All assays were performed 72 h after transfection. Transduction efficiency was confirmed via a confocal microscope. Protein/mRNA knockdown or overexpression was confirmed by western blot/qRT-PCR analysis.

2.4. Immunohistochemistry and histopathological staining

Immunohistochemistry was performed as previously described [18]. Liver sections were fixed with formalin and embedded in 5-μm-thick paraffin sections. Liver specimens were incubated with antibodies against NRP-1 (Invitrogen, Carlsbad, CA, USA), VEGFR2 (Cell Signalling Technology, Boston, MA, USA), CD31, and α-SMA (Abcam, Cambridge, UK). H&E staining was used to visualise histopathological structures (Servicebio, Wuhan, CN). Masson staining depicted the fibrotic strands in blue, and the intensity of the colour was associated with the degree of fibrosis (Servicebio, Wuhan, CN).

2.5. Western blot

Human and mouse liver samples or cells were harvested and washed twice with phosphate-buffered saline (PBS) and then lysed with 1× sodium dodecyl sulphate (SDS) loading buffer. Equal sample quantities were electrophoresed on SDS–PAGE gels and transferred onto PVDF membranes. The membranes were blocked for 1 h with 5% (w/v) skimmed milk, incubated with the primary antibodies overnight at 4 °C, and with the secondary antibodies for 1 h at room temperature. The following primary antibodies were included: anti-NRP-1 antibody (1:1000), anti-VEGFR2 antibodies (1:100), anti-CD31 antibodies (1:500), anti-α-SMA antibodies (1:500, antibody acquired from Abcam); anti-Akt/pAkt antibody (1:1000), anti-ERK/pERK antibody (1:1000), anti-PI3K/pPI3K antibody (1:1000), anti-PLCγ-1/pPLCγ-1 antibody (1:1000), and anti-FAK/pFAK antibody (1:1000, acquired from CST). Anti-β-actin antibody (1:1000), anti-GAPDH antibody (1:1000) or anti-β-tubulin antibody (1:1000, acquired from CST) were used as an internal control in different experiments, respectively. Western blot results were quantified using ImageJ software (National Institutes of Health, Bethesda, MD, USA). β-actin, GAPDH or β-tubulin in the same membrane were used as internal controls. All the antibody bands were normalized to their expression.

2.6. qRT-PCR

Human and mouse liver samples or cells were harvested, total RNAs were isolated with an RNA kit (Tiangen, Beijing, CN), and cDNAs were generated with a reverse transcription kit (Takara, Kusatsu, Japan). Gene expression was determined with real-time-PCR using SYBR Green PCR kit (Takara, Kusatsu, Japan). Real-time fluorescence monitoring was performed with the Roche480 Real Time PCR System instrument. Human and mouse NRP-1, VEGFR2, as well as human CD31, α-SMA, collagen1αI (col1), fibronectin (FN), and FAK mRNAs were normalized to GAPDH or 18S ribosomal RNA (rRNA), with results shown as fold of control. The sequences for reverse transcription primers and real-time PCR are listed in Supplementary materials (Supplement Table 2).

2.7. Vascular tube formation assay

After lentiviral transduction, cells were seeded at a density of 1×10^4 cells/ml on 50 μl Matrigel after 30 minutes of preincubation at 37 °C. Experiments were performed in the presence or absence of exogenous VEGFA-165 (10 ng/ml, Peprotech, NJ, USA) or sNRP-1 (50 μg/ml, Abcam, Cambridge, UK) or NRP-1 inhibitor (MCE, NJ, USA) or another inhibitor for 4–8 h at 37 °C and 5% CO_2. Cells were photographed using a phase-contrast microscope (Nikon USA, Garden City, NY, USA) at 100× magnification. Tube formation was quantified by counting the average number of tubes in four randomly selected fields and analysing them using the Image-Pro Plus software (Media Cybernetics, Madrid, USA).

2.8. Endothelial cell migration assay

Cell migration was measured by Transwell assays. Cells were briefly suspended in medium supplemented with 1% FBS and incubated for 30 min with or without treatment. A total of 10^4 cells were added to the upper side of each insert and inserts were then placed in 24-well plates containing medium supplemented with or without VEGF-A165 (10 ng/mL). Plates were incubated for 24 h at 37 °C in an atmosphere containing 5% CO_2, and after the times indicated, the number of cells that had migrated to the lower surface of the filters was evaluated. An average of at least four measurements per condition from two individual wells were analysed for each experiment.

2.9. Proliferation assay

The relative proliferation rates of HUVECs transduced with either lentivirus or control were determined by cholecystokinin-8 (CCK-8) assay. HUVECs were seeded in 96-well plates at 5000 cells/well and left to adhere overnight. After a 24-h cell culture, 10 μl of CCK-8 (MCE) was added to each culture well and incubated for 1 h. Optical density (OD) was measured at 450 nm using a scanning multi-well spectrophotometer (Bio-Rad Model 550, CA, USA). The cell viability rate was calculated using the following equation: cell viability rate = [(OD lentivirus group – OD control group)/OD lenti-control group – OD control group] × 100%. All experiments were performed in triplicate and repeated three times.

2.10. Liver histocultures

Human liver tissue specimens were obtained from surgical resections. Fibrotic liver tissue beyond the edge of the abnormality was collected from 4 hepatocellular carcinoma(HCC) patients with similar liver fibrosis stages and degrees of liver function. In liver histoculture, 4 samples from 4 HCC patients were used, with three sub-wells for each treated group of each sample. The tissues were then transported to the laboratory in PBS with 1% antibiotics. The tissue was washed three times, dissected in PBS, and then gently cut into pieces of approximately 2–3 mm^3 in size. Four pieces were placed on a 1 cm^3 sponge (Vetspon, IN, USA) which was inserted into the well of a 12-well dish (Corning, NY, USA). The pieces were submerged in 1640 nutrient mixture (1.5 ml per well) and supplemented with 10% FBS, 1% insulin, and 2% hydrocortisone. The dish was placed in an incubator chamber with 5% CO_2 and then incubated at 37 °C. After a 24-h incubation period, the medium was changed and treated with NRP-1 inhibitor in different concentrations and the procedure was repeated every 24 h. At the end of the 7-d incubation, one piece of fresh tissue was collected for CCK-8 tests to assess tissue viability, using the following the formulas: Tissue viability rate (%) = [(Absorbance/g of tumour in the treated group)]/ [(Mean of absorbance/g of tumour in the untreated group)] × 100 [19]. Other fresh tissue samples were collected for qRT-PCR analyses or were fixed in 10% buffered formalin for immunohistochemistry and histological staining. GAPDH and 18S rRNA were used as an internal control for qRT-PCR.

2.11. Statistical analysis

All statistical analyses were carried out with SPSS version 22.0 software (SPSS, Chicago, IL, USA). Experiments were performed at least three independent times. Numerical data were expressed as the means ± standard deviation (SD) and categorical data were expressed as numbers (percentages). The differences between groups were analysed by paired and unpaired 2-tailed Student's t test or by an ANOVA, as deemed appropriate. The Spearman rank correlation coefficients of determination was used to analyse the degree of correlation among parameters. For all analyses, the p-value reported was two-tailed, and p-values < .05 were considered statistically significant.

3. Results

3.1. NRP-1 expression was significantly increased in HSECs during cirrhosis and was positively correlated with VEGFR2 expression and intrahepatic angiogenesis levels

The expression of NRP-1 was first examined in human cirrhotic liver tissue and normal liver tissue by immunohistochemistry. The degree of cirrhosis in liver samples was confirmed by H&E and Masson staining (Fig. 1A). As shown in Fig. 1A, NRP-1 was positively stained primarily along the sinusoids and confined in HSECs, while co-distributing with VEGFR2 staining. The levels of intrahepatic angiogenesis and fibrosis

in cirrhotic individuals were tested by immunohistochemistry staining with an endothelial cell-specific anti-CD31 antibody and an anti-α-SMA antibody. Both NRP-1 and VEGFR2 expressions in the cirrhotic liver tissue were elevated along with intrahepatic and fibrosis levels. Also, we found that the NRP-1 and VEGFR2 expression was significantly upregulated in cirrhotic liver tissue compared to normal liver tissue, as demonstrated by western blot results (Fig. 1B and C, 0.56 ± 0.11 vs. 0.15 ± 0.05, p = .0219 and 0.44 ± 0.08 vs. 0.06 ± 0.01, p = .0067, respectively) and qRT-PCR analyses (Fig. 1D, 11.91 ± 2.88 vs. 0.83 ± 0.10, p = .0193, 3.50 ± 0.86 vs. 0.78 ± 0.15, p = .0446, respectively).

To evaluate the role of NRP-1 expression in the progression of cirrhosis, CCl$_4$-administered mice cirrhosis models were constructed and used for the following experiments. H&E and Masson staining showed the time course of the nodular changes and the subsequent deposition of collagen fibres, suggesting that cirrhosis models were created successfully (Fig. 2A). The expression of NRP-1, VEGFR2, and angiogenesis and fibrosis markers in mouse livers of control (n = 4) and CCl$_4$-treated 6 or 8 week groups (n = 5) were confirmed by immunohistochemistry staining (Fig. 2A), western blotting (Fig. 2B, p < .05), and

qRT-PCR analysis (Fig. 2C, p = .0023 and p = .0147, respectively). The expression of NRP-1 was upregulated in conjunction with VEGFR2 (Fig. 2D, R = 0.829, p = .0003) and correlated positively with the levels of intrahepatic angiogenesis (Fig. 2E, R = 0.783, p = .0009) during cirrhosis progression. Thus, the results from mice and human cirrhosis analyses support the potential pathobiological significance of NRP-1, which aggravates liver cirrhosis by promoting intrahepatic angiogenesis in HSECs, based on the upregulation of its expression and distribution with VEGFR2.

3.2. NRP-1 promoted angiogenesis of HSECs

As the expression of NRP-1 increased in HSECs in cirrhotic liver tissue, we examined whether NRP-1 could modulate HSEC angiogenesis in vitro. Human HSECs and HUVECs were used to decipher the effects of endothelial NRP-1 on the modulation of angiogenesis with gain-of-function and loss-of-function approaches in combination with tube formation, migration, and proliferation assays. NRP-1 was knocked down by using lentivirus and NRP-1-knockdown efficiency was confirmed
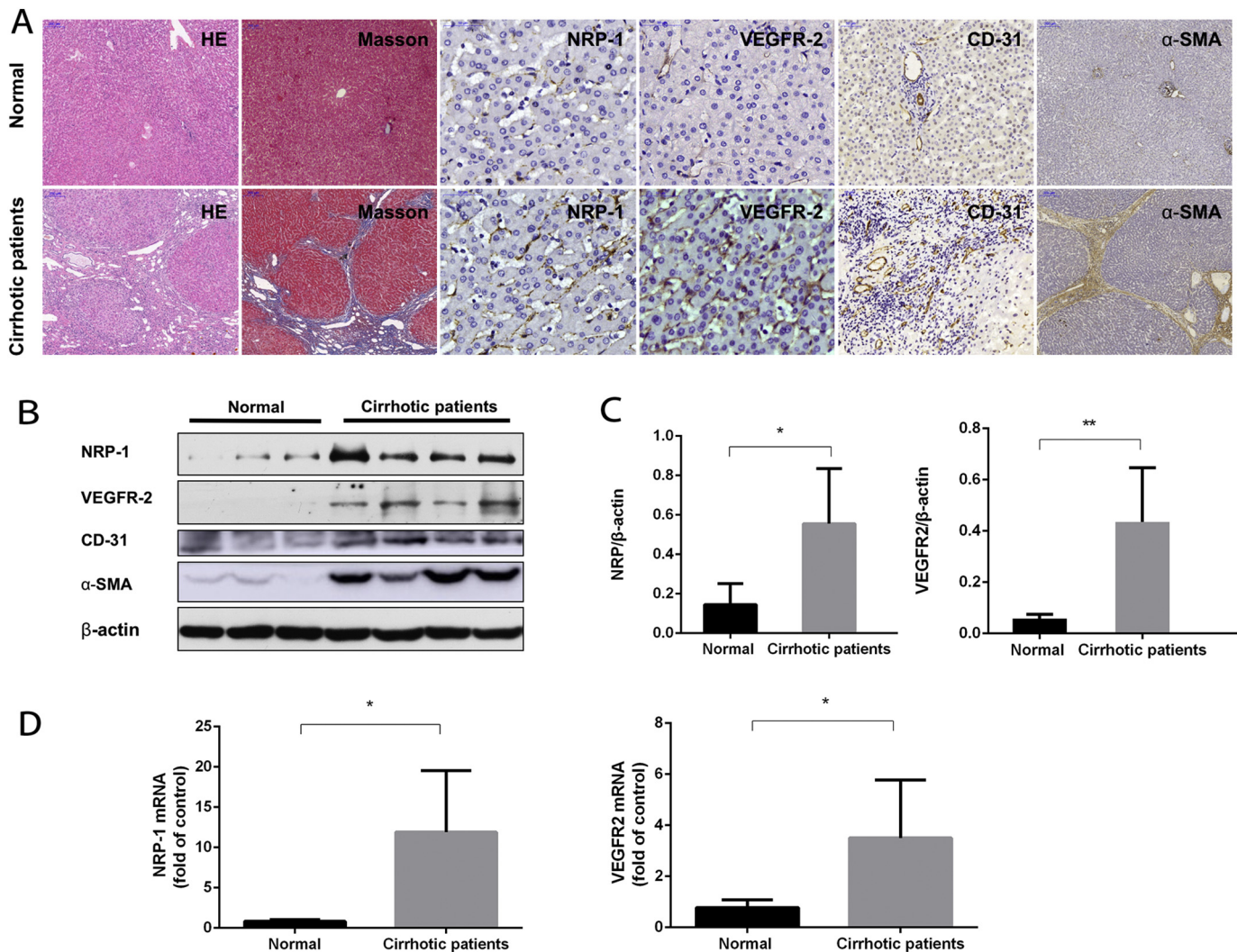

Fig. 1. NRP-1 upregulation in the HSECs is consistent with the enhancement of intrahepatic angiogenesis and fibrosis in human cirrhotic livers. (A) Representative histopathology images of human liver tissues with H&E staining (×50; scale bar = 200 μm), Masson staining (×50; scale bar = 200 μm), and immunohistochemistry images for NRP-1, VEGFR2, CD31, and α-SMA are shown for the normal group (up panels, n = 3) and the cirrhotic patients group (down panels, n = 7). NRP-1 and VEGFR2 were stained along the sinusoids, (×400; scale bar = 50 μm), CD31 in the intimal lining of the microvessels (×100; scale bar = 50 μm), and α-SMA in liver scar tissue appeared as brown deposits (×50; scale bar = 50 μm). (B) Western blotting showed that NRP-1, VEGFR2, CD31, and α-SMA protein levels in livers from cirrhotic patients were elevated compared with those in the normal group. (C) Both NRP-1 and VEGFR2 protein content were increased in human cirrhotic liver samples as assessed by western blotting (p = .0219 and p = .0067, respectively. **p < .01, *p < .05). (D) NRP-1 and VEGFR2 mRNA levels were analysed and compared in liver samples of cirrhotic patients and a control group. Both molecules were increased in human cirrhotic liver samples as assessed by qRT-PCR (p = .0193 and p = .0446, respectively. *p < .05). (For interpretation of the references to colour in this figure legend, the reader is referred to the web version of this article.)
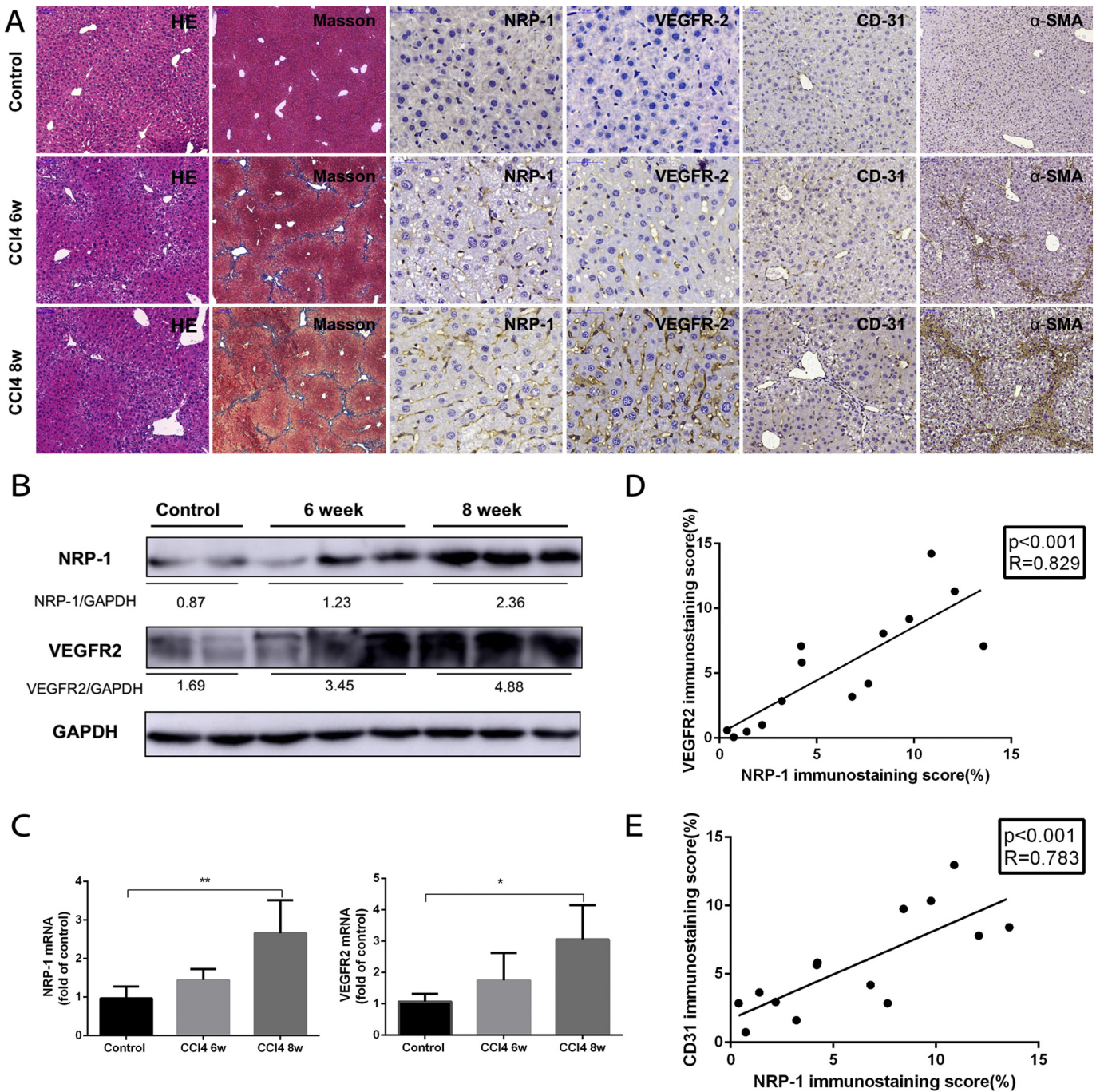
Fig. 2. NRP-1 expression is positively correlated with VEGFR2 expression and intrahepatic angiogenesis during cirrhosis progression in a cirrhotic mice model. (A) Time course expression of NRP-1 in control group mice livers (n = 4) and the CCl₄-treated group over 6 or 8 weeks (n = 5). Liver tissues of mice treated with CCl₄ were stained with H&E (×100; scale bar = 100 μm) and Masson (×50; scale bar = 200 μm) and immunostained using NRP-1 (×400; scale bar = 50 μm), VEGFR2 (×400; scale bar = 50 μm), CD31 (×200; scale bar = 100 μm), and α-SMA ab (×100; scale bar = 500 μm). (B) Western blotting showed that NRP-1, VEGFR2, CD31, and α-SMA protein levels in CCl₄-treated mice livers were increased in relation to the stage of cirrhosis. (C) NRP-1 and VEGFR2 mRNA levels were increased in accordance with the stage of cirrhosis of CCl₄-treated mice liver samples by qRT-PCR (p = .0023 and p = .0147, respectively. **p < .01, *p < .05). (D) A significant correlation was observed between NRP-1 and VEGFR2 staining scores in mice liver samples (p = .0003, ***p < .001). (E) A significant correlation was observed between NRP-1 staining scores and CD31 staining in mice liver samples (p = .0009, ***p < .001).

by confocal microscope (Supplement Fig. 1A). A significant reduction of NRP-1 expression was detected by qRT-PCR and western blot analyses (Fig. 4A and C). We therefore performed the capillary-like tube formation assay in HSECs to assess NRP-1 knockdown at a functional level. The results indicated that the NRP-1-RNAi group demonstrated a significant reduction in the number of tubes compared to the lentivirus GFP control group. While VEGF increased HSECs tube formation, NRP-1-RNAi inhibited VEGF-induced angiogenesis (Fig. 3A), The same result was obtained in HUVECs, VEGF increased HUVECs tube formation

(p = .038), NRP-1-RNAi inhibited VEGF-induced tube formation (p = .0045) (Fig. 3B). In addition, cells transfected with NRP-1-RNAi showed a significant decrease in the number of migrating cells in Transwell assay compared with the control groups (Fig. 3C and D, p = .0112). Furthermore, NRP-1-RNAi-treated cells presented a modest decrease in cell proliferation via CCK-8 assay (Supplement Fig. 1C). We used an NRP-1-overexpression approach to test our hypothesis by performing lentiviral-mediated overexpression of NRP-1 (lenti-NRP-1) and lenti-control in HSECs (Supplement Fig. 1B). NRP-1 overexpression was

confirmed by a striking increase in NRP-1 expression via qRT-PCR and western blot analyses (Fig. 4B and C). The tube formation assay indicated that NRP-1 overexpression led to a significant increase in the number of tubes compared to the lenti-control group due to NRP-1 function during VEGF-induced HSEC angiogenesis (Fig. 3E); the same results were observed in HUVECs (Fig. 3F, p = .0317 and p = .0351, respectively). Moreover, the Transwell assay indicated that NRP-1 is also important for cell migration (Fig. 3G and H, p = .0272). However, there was no significant difference in the tube formation and the migration capability of lenti-NRP-1 cells in the presence or absence of VEGF (p = .644 and p = .336, respectively). In addition, lenti-NRP-1-treated cells presented a modest increase in cell proliferation via CCK-8 assay (Supplement Fig. 1D). In conjunction, these results indicate an integral role for NRP-1 in promoting angiogenesis.

3.3. NRP-1 promoted angiogenesis by upregulating VEGFR2 via FAK in HSECs

Due to the concomitant expression of NRP-1 and VEGFR2 in HSECs, we further examined whether NRP-1 modulated HSEC angiogenesis in a VEGFR2-dependent manner. It was interesting that the downregulation of NRP-1 decreased not only the phosphorylated VEGFR2 but also VEGFR2 protein and mRNA in the three EC strains (Fig. 4A and C, left panel). However, NRP-1 overexpression significantly increased phosphorylated and total VEGFR2 protein content as well as NRP-1 mRNA in ECs compared to lenti-control cells (Fig. 4B and C, right panel). In addition, in conjunction with the change of VEGFR2 levels induced by NRP-1 down/upregulation, FAK mRNA levels also significantly changed (Fig. 4D, p < .001)). Moreover, NRP-1 enhanced the total FAK and phosphorylation protein levels in HSECs (Fig. 4E). As reported by Sun, FAK and its associated kinase activity regulate VEGFR2 transcription in HUVECs [20]. Therefore, we examined the possibility that NRP-1 may regulate VEGFR2 expression via FAK in HSECs. To test this hypothesis, FAK kinase activity inhibition via PF573228 was performed in lenti-control and lenti-NRP-1 HSECs, after which cells were treated with VEGF. The increase in expression and activation of VEGFR2 induced by NRP-1 was inhibited by the FAK inhibitor(PF573228) (Fig. 4E), indicating that FAK played a key role in the NRP-1-mediated upregulation of VEGFR2 expression and activation. Collectively, these results indicate that NRP-1 further regulated VEGFR2 expression at transcriptional and post-translational levels via the upregulation of FAK and its kinase activity.

3.4. NRP-1 increased VEGFR2-dependent angiogenesis via the PI3K/Akt pathway in HSECs

We next sought to figure out whether VEGFR2-dependent downstream signalling pathways were affected by NRP-1. First, HUVECs were treated with VEGF for differing periods (0, 5, 10, 15, 30, and 60 min) and then collected to examine the various signalling intermediates present via western blotting. VEGF-induced VEGFR2 activation and its downstream signals with peak phosphorylation were observed at 15 min and declined to baseline levels after 60 min (Supplement Fig. 1E). Therefore, 15 min was chosen as the intercept time to further identify the NRP-1-affected signalling pathways in control and lentivirus-NRP-1-transfected HUVECs. Along with the phosphorylation of VEGFR2, lenti-NRP-1 increased VEGF-induced PI3K/Akt and PLCγ-1/ERK1/2 activation in HUVECs compared with control cells (Fig. 5A and B, p = .022, p = .048, p = .039, p = .024, p = .021, respectively). In order to determine which signalling pathway was involved in NRP-1-mediated modulation of angiogenesis, both the PI3K inhibitor (LY294002) and MEK inhibitor (PD98059) were used in lenti-NRP-1 and lenti-control transfected HUVECs. The results indicated that in both lenti-NRP-1 and lenti-control HUVECs, LY294002 inhibited the NRP-1-mediated phosphorylation of Akt (Supplement Fig. 2A) and angiogenesis (Supplement Fig. 1F and Fig. 5C, p < .05). Similar experiments

were repeated in HSECs and the same results were obtained, indicating that NRP-1 modulated VEGFR2-dependent angiogenesis through the PI3K/Akt pathway in ECs (Fig. 5D and E, p = .0286, p = .047 and p = .0318, respectively).

3.5. Blocking NRP-1 function inhibits neoangiogenesis and fibrosis in fibrotic liver histoculture in vitro

The expression of NRP-1 was upregulated in the lenti-NRP-1 group compared with the lenti-control group, as confirmed via western blotting in HSECs (Supplement Fig. 2B). Both the NRP-1 inhibitor (EG00229) and sNRP-1-targeting-NRP-1 inhibited angiogenesis of HSECs in vitro (Supplement Fig. 1G, Fig. 6A, p < .05). Given these results, we hypothesized that the administration of an NRP-1 inhibitor might also modulate angiogenesis in fibrotic liver histocultures. Liver tissues from fibrotic patients obtained from liver surgeries were cultured on sponges, followed by a daily administration of NRP-1 inhibitor for 1 week at varying concentrations (0, 10, 20, 50 μM). The survival rates of all cultured fibrotic tissues were tested via CCK-8 assay. Fibrotic tissue treated with the NRP-1 inhibitor showed an increased survival rate compared with vehicle-treated tissue, in a manner that was concentration-dependent (Fig. 6B, p < .001). Although Masson staining of liver histopathological structures indicated a similar trend, no significant differences were found between vehicle and NRP-1-inhibitor treated groups, which was most likely due to the short treatment time (Fig. 6C, p > .05). The difference in neoangiogenesis between vehicle and NRP-1-inhibitor treated tissue was evidenced by the quantification of CD31 mRNA (Fig. 6D, p = .0019). Importantly, in addition to reduced neoangiogenesis, fibrotic tissue treated with NRP-1 inhibitor also showed a reduced severity of liver fibrosis factors compared with vehicle-treated tissue as measured by the quantification of α-SMA, Fn, and Col1 mRNA levels (Fig. 6E–H, p = .0002, p = .048, p = .0195, respectively, and Supplement Fig. 2C–F).

4. Discussion

Liver cirrhosis, which eventually results in oesophageal varices, ascites, and HCC, accounts for the majority of morbidity and mortality rates in patients with chronic liver disease and has limited treatment options available. In this study, we demonstrated that NRP-1 played a vital role in promoting HSEC-induced intrahepatic angiogenesis in both human and rodent liver cirrhosis. In vitro, we found that NRP-1 modulated VEGFR2 function by regulating FAK and its kinase activity, while further promoting VEGFR2-dependent intrahepatic angiogenesis through its downstream PI3K/Akt signal pathway, as shown in the proposed model (Fig. 7). Furthermore, blocking NRP-1 reduced intrahepatic angiogenesis and fibrosis-associated factors in liver tissue cultures. In conclusion, we highlight the significance of NRP-1 as a therapeutic target for the treatment of liver cirrhosis.

At present, intrahepatic angiogenesis has increasingly been associated with the development of cirrhosis. In this study, we found that the expression of NRP-1 was upregulated in cirrhosis, which was consistent with the enhancement of the degree of intrahepatic angiogenesis and fibrosis (Figs. 1 and 2). Previous studies, including our own, have demonstrated that intrahepatic angiogenesis induced by HSECs was positively correlated with fibrosis induced by HSCs, although the mechanistic relationship between these two processes was not fully defined [10,21,22]. Research by Liu et al. illuminated the stage-dependent role of HSEC-induced angiogenesis and angiogenesis-induced activation of HSC in mechanotransduction-modulated fibrotic microniches [23]. In this study, we found that NRP-1 was highly expressed on HSECs and played a vital role in intrahepatic angiogenesis, in conjunction with liver fibrosis, during cirrhosis progression. Recent studies, including our earlier results, indicated that NRP-1-induced HSCs-derived fibrosis through PDGF and TGF-β pathways and that targeting NRP-1 by an inhibitory NRP-1 antibody reduced fibrogenesis markers and inhibited
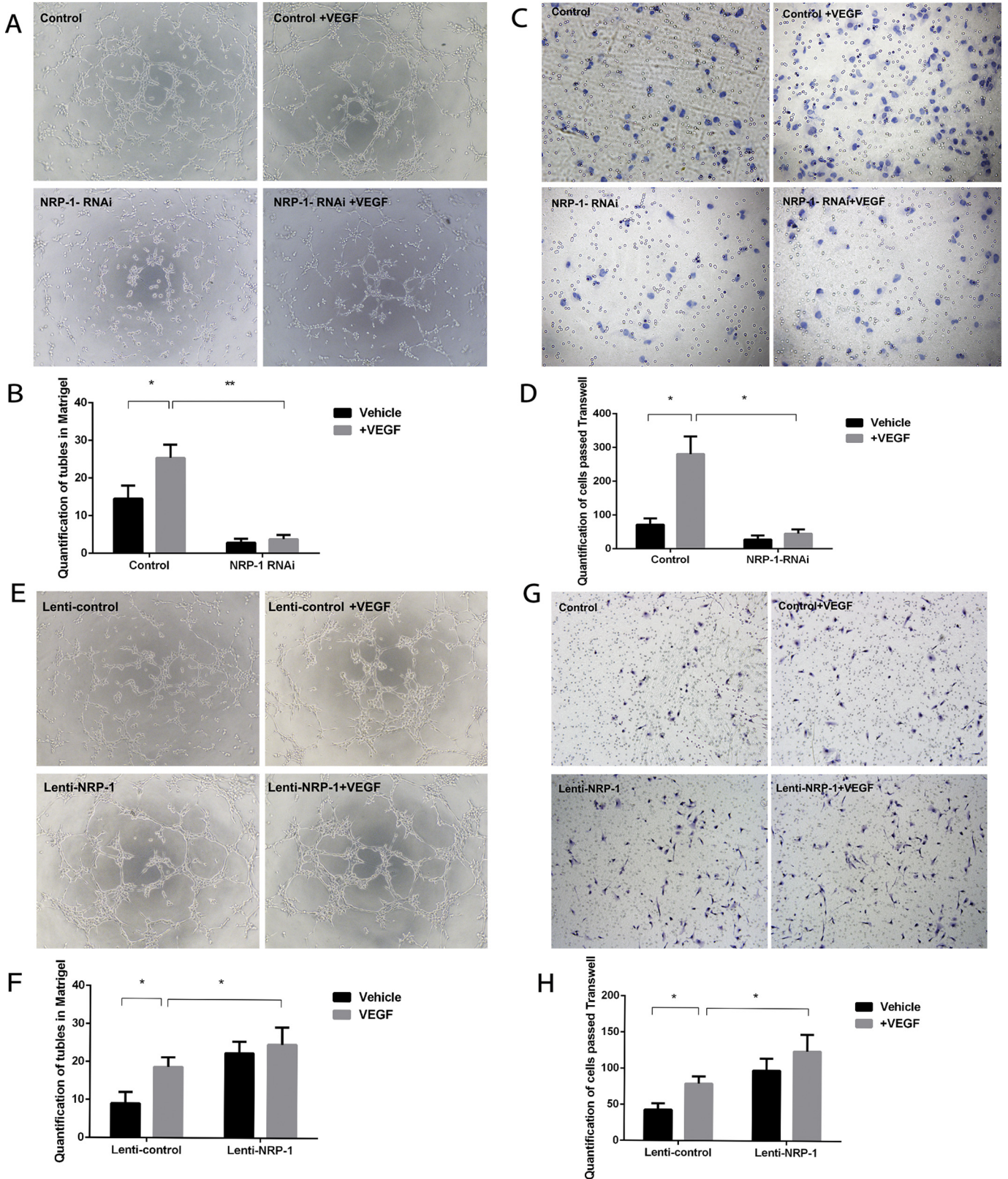
Fig. 3. NRP-1 is required for HSECs capillary-like tube formation and cells migration in vitro. NRP-1 was downregulated or overexpressed with lentivirus in HSECs and HUVECs. (A) HSECs transfected with lentivirus NRP-1-RNAi showed diminished angiogenesis compared to cells transfected with the control via a tube formation assay and also showed impaired responses to VEGF. (B). Quantification of tubes in Matrigel was measured in NRP-1-RNAi and control groups in the presence of either vehicle or VEGF in HUVECs (n = 3, p = .038 and p = .0045, respectively. **p < .05, *p < .05). (C). Cell migration was also studied using Transwell assay in HSECs transfected with lentivirus NRP-1-RNAi or lentivirus control. Cells transduced with lentivirus NRP-1-RNAi showed decreased VEGF-dependent cell movement in comparison to cells transduced with lentivirus control. (D) The quantification of HUVECs that passed through the Transwell filter in different groups is shown (n = 3, p = .0112 and p = .0107, *p < .05). (E) HSECs transduced with lenti-NRP-1 showed enhanced tube formation compared with the lenti-control. (F) The quantification of HUVECs in tubes of Matrigel in the lenti-NRP-1 and lenti-control groups are shown (n = 3, p = .0317 and p = .0351, *p < .05). (G) Migration of HSECs in lenti-NRP-1 group increased in comparison with the lenti-control group. (H) The quantification of data in terms of number of HUVEC migrations was measured (n = 3, p = .0125 and p = .0272, *p < .05).
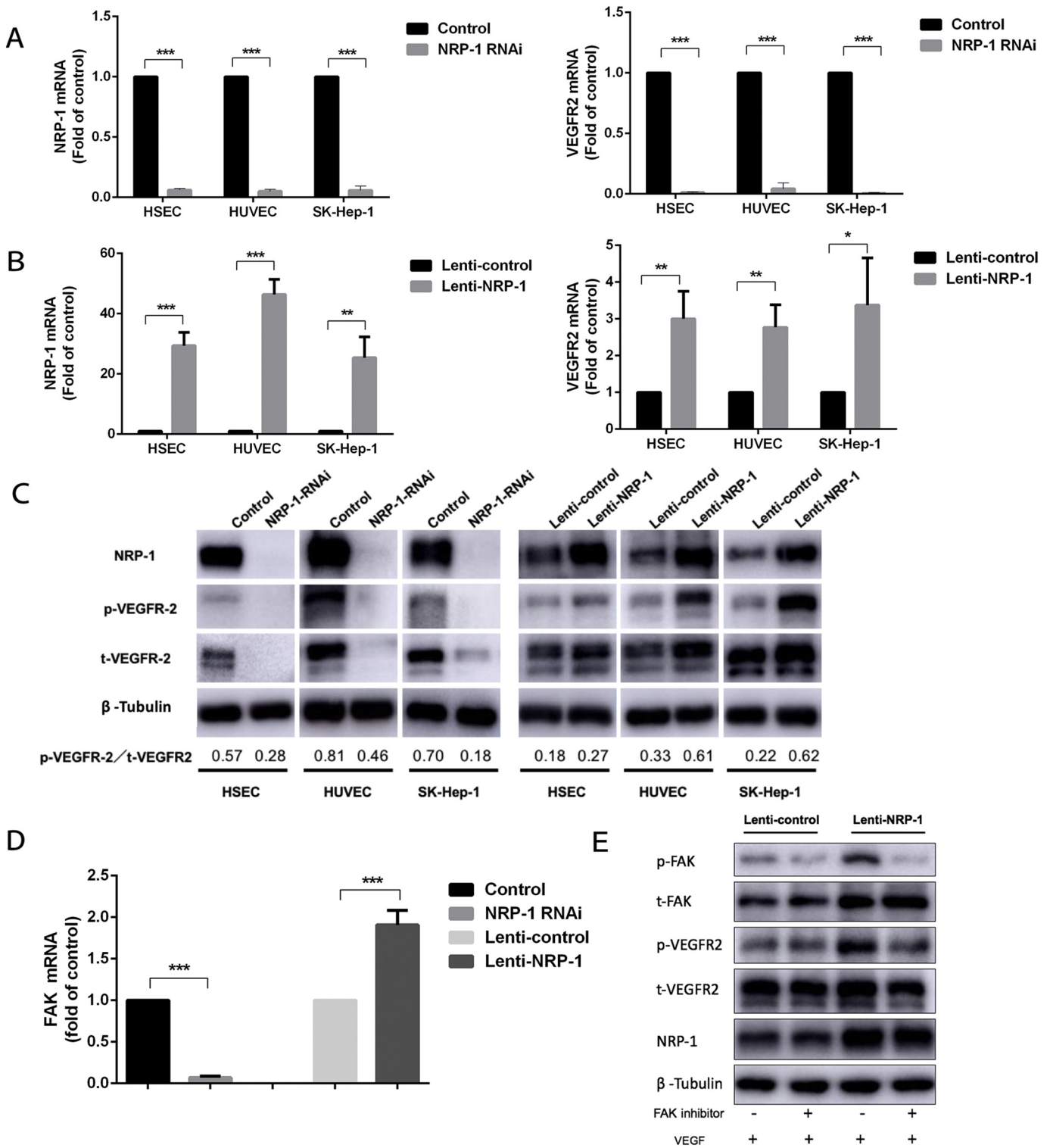
Fig. 4. NRP-1 upregulates VEGFR2 expression and activation via FAK and its activity. NRP-1 was downregulated or overexpressed with lentivirus in HSECs, HUVECs, and SK-HEP-1 cells. (A) NRP-1 mRNA was downregulated by NRP-1-RNAi compared with the control as confirmed by qRT-PCR (left, ***p < .001). Consistent with the decreased amount of NRP-1 mRNA, VEGFR2 mRNA expression was also decreased in ECs as confirmed by qRT-PCR (n = 3, ***p < .001). (B) NRP-1 mRNA was upregulated in lenti-NRP-1 group compared with lenti-control group as confirmed by qRT-PCR (left, p < .001, p < .001and p = .0037, respectively. ***p < .001, **p < .01). Consistent with the increased amount of NRP-1 mRNA, VEGFR2 mRNA expression also increased in ECs as confirmed by qRT-PCR (right) (n = 3, p = .0098, p = .0076 and p = .0331, respectively. **p < .01, *p < .05) (C) NRP-1 downregulation induced a significant reduction in the total level of VEGFR2 protein and phosphorylated VEGFR2 protein at Tyr1175 in ECs as confirmed by western blotting (left panel). NRP-1 overexpression enhanced the expression and phosphorylation of VEGFR2 at Tyr1175 as confirmed by western blotting (right panel). (D) Consistent with the changes in NRP-1 and VEGFR2 mRNA, the FAK mRNA level significantly decreased in HSECs transfected with NRP-1 RNAi compared with the control. In addition, FAK mRNA levels also increased in HSECs transfected with lenti-NRP-1 RNAi compared with the lenti-control (***p < .001). (E) NRP-1 overexpression enhanced the expression and phosphorylation of FAK at Y397 as seen in the western blot results. FAK inhibition blocks NRP-1–induced increases in the level of VEGFR2 expression and activation. (Representative WB are from three independent experiments).
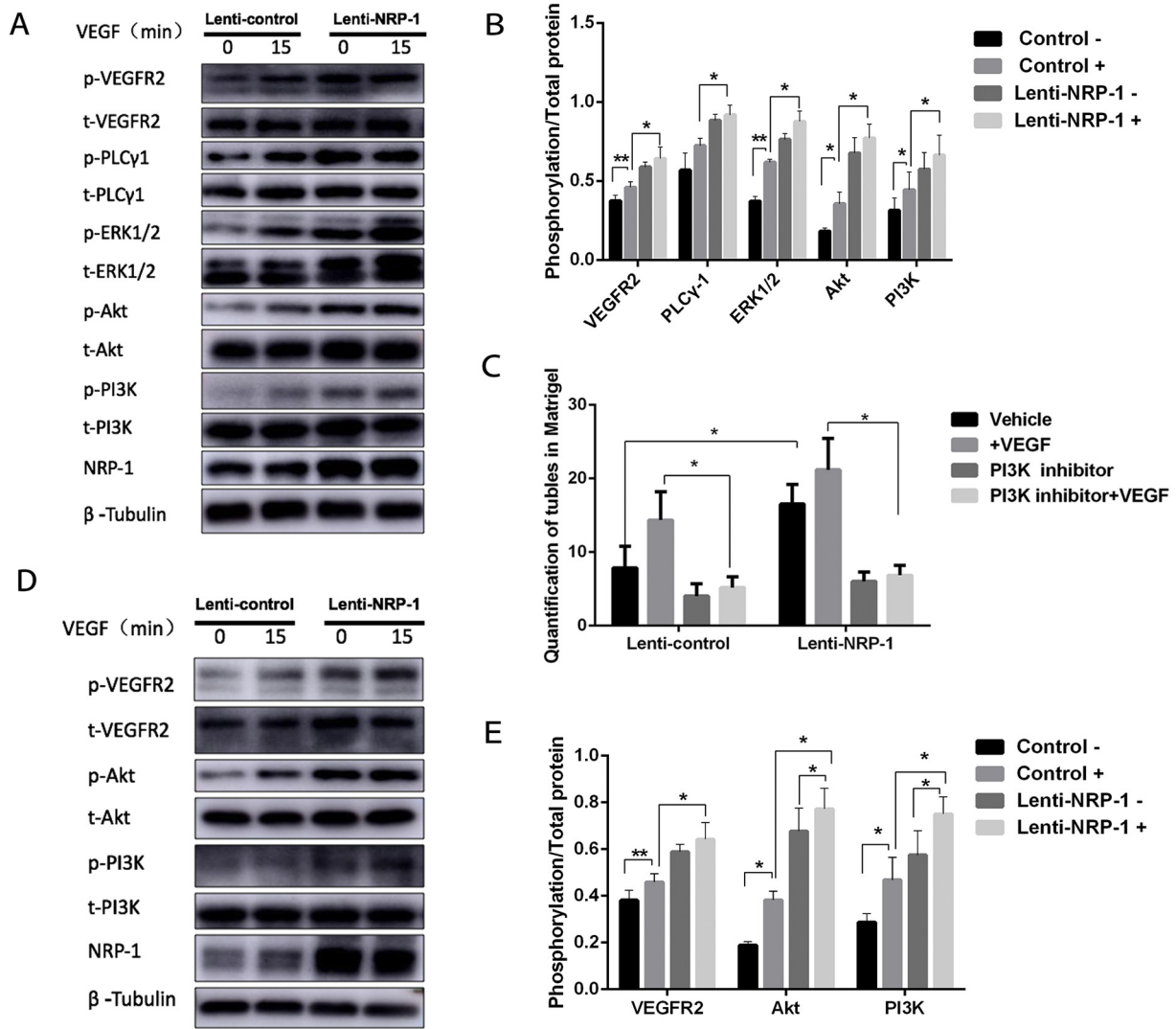
Fig. 5. NRP-1 enhances VEGFR2 phosphorylation and downstream PI3K/Akt pathway activity. (A) HUVECs transduced with lenti-NRP-1 or lenti-control were stimulated with VEGF165 (10 ng/ml) for 0 and 15 min. NRP-1 overexpression enhanced the expression and phosphorylation of VEGFR2, as well as the phosphorylation of PI3K/Akt and PLCγ-1/ERK1/2 (representative WB are from 3 independent experiments). (B) PI3K/Akt and PLCγ-1/ERK1/2 activation levels increased in HSECs cells transduced with lenti-NRP-1 compared with HUVECs cells transduced with the lenti-control (n = 3, **p < .01, *p < .05). (C) Tube formation was analysed in HUVECs transduced with lenti-NRP-1 or the lenti-control. The PI3K inhibitor blocks NRP-1-induced increases in tube formation in the presence of either vehicle or VEGF (n = 3, **p < .01, *p < .05). (D) HSECs transduced with lenti-NRP-1 or the lenti-control were stimulated with VEGF165 (10 ng/ml) for 0 and 15 min. NRP-1 overexpression enhanced the expression and phosphorylation of VEGFR2, as well as the phosphorylation of PI3K/Akt. (Representative WB are from three independent experiments). (E) VEGFR2 and PI3K/Akt activation levels were increased in HSECs cells transduced with lenti-NRP-1 compared with HSECs cells transduced with the lenti-control (n = 3, **p < .01, *p < .05).

fibrosis [10,24]. As HSEC-induced intrahepatic angiogenesis and HSC-induced fibrosis collaboratively drive liver cirrhosis, defining the role of NRP-1 in HSEC-induced angiogenesis could have potential therapeutic effects on cirrhosis, analogous to hitting two birds with one stone.

Our study was particularly focused on the modulating function of NRP-1 on intrahepatic angiogenesis in HSECs, especially by regulating VEGFR2. As mentioned previously, NRP-1 is a transmembrane protein with a very short intracellular domain that lacks enzymatic activity. Therefore, it is well-accepted that NRP-1 mediates functional responses by forming a VEGF-dependent complex with VEGFR2 to facilitate angiogenesis [13,14]. However, several studies have suggested that NRP-1 could also act on angiogenic endothelial cells in a VEGF-independent manner [15,16]. In our study, we confirmed that NRP-1 controlled the expression and activation of VEGFR2 in ECs. The report by Gelfand is consistent with our results indicating that NRP-1 might control vascular development by directly modulating VEGFR2 in NRP-1 fl/− mutant animal experiments [15]. It is worth noting that while we found that NRP-1 modulated VEGFR2 at both the transcriptional and protein levels in HSECs (Fig. 4), other studies have demonstrated that downregulation

of NRP-1 decreased VEGFR2 protein levels but not mRNA levels by modulating VEGFR2 trafficking through the stabilization of cells on the surface [25–27], which is probably due to the different sources and types of ECs.

According to our results, both mRNA and protein levels of VEGFR2 were synchronously altered by the change of NRP-1, which was accompanied by the expression of FAK in HSECs. In addition, NRP-1 overexpression enhanced the expression and phosphorylation of FAK at Y397. Recent findings suggest that the binding of VEGF to NRP-1 is important for FAK Tyr-407 phosphorylation in endothelial cells, and the mechanism for NRP-1 regulation of FAK requires further study. Meanwhile, the inhibition of FAK could block the NRP-1-induced increase of VEGFR2 expression. Recently, a study by Sun indicated that FAK directly participated in the transcriptional regulation of VEGFR2, as evidenced by the detection of nuclear FAK in the RNA polymerase II complex associated with VEGFR2 [20]. Therefore, we speculate that FAK served as an intermediate molecule in the NRP-1-induced modulation of VEGFR2.

Together, we suggested that NRP-1 may regulate VEGFR2 expression at the transcriptional and posttranslational levels by upregulating FAK
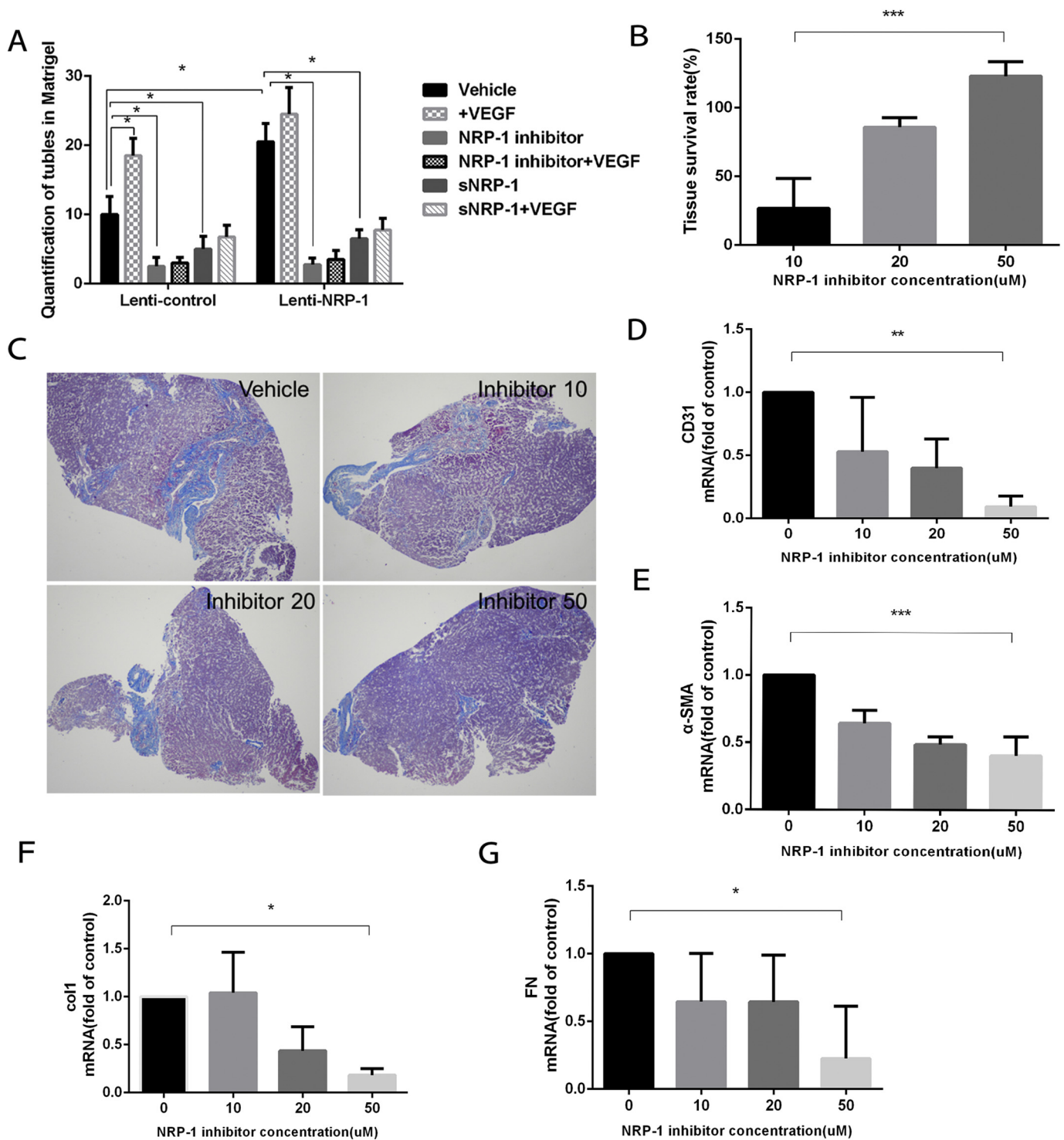
Fig. 6. Blocking NRP-1 function inhibits neoangiogenesis and fibrosis in vitro fibrotic liver tissue culture. (A) EG00229, a pharmacologic inhibitor of NRP-1 and sNRP-1, is a competitive soluble protein inhibitor of NRP-1 and was able to block enhanced angiogenesis conferred by lenti-NRP-1 overexpression in HSECs (n = 3, *p < .05). (B) Fibrotic liver tissues of patients administered vehicle (n = 4) or EG00229 (n = 4) in various drug concentrations (0,10 20,50 μM) were tested by CCK-8 after culturing for 7 days. The EG00229-treated fibrotic tissue showed an increased survival rate compared with vehicle-treated tissue, in relation to the drug concentration. (***p < .001) (C) Representative images for Masson staining in each liver tissue sample showed no significant differences between different treatment groups (original magnification, 40×). (D) Angiogenesis markers were quantified from the tissue sections in each group using qRT-PCR, with GAPDH as internal control. CD31 mRNA levels were significantly reduced in tissues treated with EG00229 compared with control tissues (p = .0019, **p < .01). (E–G) Fibrosis markers were also quantified using qRT-PCR, with GAPDH as internal control, from tissue sections pertaining to each group. Results showed that α-SMA, collagen1α I, and FN mRNA levels were significantly reduced in tissue treated with EG00229 compared with control tissues (p = .0002, p = .048, p = .0195, respectively. ***p < .001, *p < .05).

and its kinase activity. In this manner, NRP-1 acts as an important regulator of angiogenesis by controlling the degree and activation of VEGFR2.

The activation of VEGFR2 initiates multiple intracellular signal transduction pathways that regulate endothelial survival, proliferation, migration, and lumenization [17,18] that involve p38, ERK1/2, PI3K/Akt,
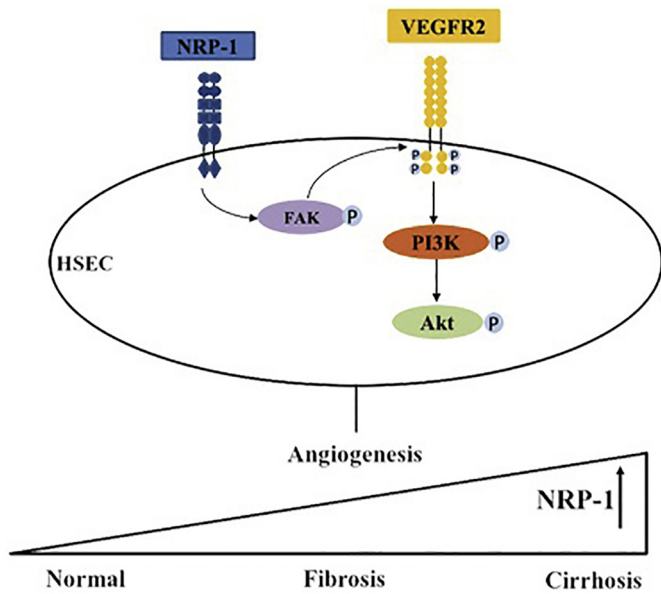
Fig. 7. Mechanistic role of NRP-1 in intrahepatic angiogenesis of liver cirrhosis. A proposed model depicting the role of NRP-1 in intrahepatic angiogenesis of liver cirrhosis. NRP-1 upregulates the expression and activation of VEGFR2 at transcriptional and post translational levels through upregulating FAK and its kinase activity. Furthermore, NRP-1 promotes intrahepatic angiogenesis by amplifying VEGFR2 phosphorylation and the downstream PI3K/Akt signalling pathway. Increases in NRP-1 correspond with liver cirrhosis progression and support the potential role of this molecule as a therapeutic target for liver cirrhosis treatment.

and Src/FAK. In the present study, we found that the phosphorylation of VEGFR2 also activated a ERK1/2 signalling cascade; however, inhibiting ERK1/2 activation did not significantly inhibit EC tube formation (data not shown), indicating that PLCγ-1/ERK1/2 pathways may not be involved in this process. This result is reasonable as a portion of the data reveal that VEGF-driven activation of ERK1/2 signalling is critical for both developmental and adult arteriogenesis [28]. In the former study, the activation of PI3K/Akt was reported to promote endothelial cell survival by inhibiting apoptosis [29]; in this study, we further identified that the PI3K/Akt signalling pathway promotes endothelial cell tube formation (Fig. 5C and D). However, the mechanistic studies were performed in endothelial cell cultures without a cirrhotic environment. Further study in liver histocultures and cirrhotic animal models are needed to verify these results in vitro.

Due to the critical role of NRP-1 in angiogenesis in cirrhosis, liver histocultures were used to test the therapeutic effect of NRP-1 in human cirrhotic liver biopsies to simulate the environment of the human liver. We found that by blocking NRP-1 function with an NRP-1 inhibitor in liver histocultures, a decrease in angiogenesis and fibrosis markers were observed. Correspondingly, our cell culture experiments also demonstrated that siNRP-1 and NRP-1 inhibitor treatments suppressed the tube formation of cultured HSECs (Fig. 6A and Supplement Fig. 1E). It is worth noting that a human anti-NRP-1 antibody targeting both angiogenesis and fibrosis is under clinical evaluation as a cancer treatment [30]. Collectively, NRP-1 could be an important therapeutic target due its duel anti-angiogenesis and anti-fibrosis effects, especially for patients resistant to VEGF-targeting drugs.

Supplementary data to this article can be found online at https://doi.org/10.1016/j.ebiom.2019.04.050.

Acknowledgments and funding sources

Declaration of interests

The authors do not have a commercial or other association with pharmaceutical companies or other parties that might pose a conflict of interest.

Authors' contributions

Literature search: Le Wang, Yuemin Feng;
Figures: Le Wang, Xiaoyu Xie;
Study design: Le Wang, Hao Wu, Jianni Qi;
Data collection: Le Wang, Xiaoyu Xie;
Data analysis: Le Wang, Xiaonan Su;
Data interpretation: Le Wang, Qiang Zhu;
Writing original draft: Le Wang;
Writing draft: Le Wang，Yuemin Feng，Qiang Zhu, Wei Xin, Ying Zhang, Lifen Gao, Vijay H. Shah.

References

[1] Schuppan D, Afdhal NH. Liver cirrhosis. Lancet 2008;371(9615):838–51.
[2] Iwakiri Y, Shah V, Rockey DC. Vascular pathobiology in chronic liver disease and cirrhosis - current status and future directions. J Hepatol 2014;61(4):912–24.
[3] DeLeve LD. Liver sinusoidal endothelial cells in hepatic fibrosis. Hepatology 2015;61(5):1740–6.
[4] Ferrara N, Gerber HP, LeCouter J. The biology of VEGF and its receptors. Nat Med 2003;9(6):669–76.
[5] He Z, Tessier-Lavigne M. Neuropilin is a receptor for the axonal chemorepellent Semaphorin III. Cell 1997;90(4):739–51.
[6] Bielenberg DR, Pettaway CA, Takashima S, Klagsbrun M. Neuropilins in neoplasms: expression, regulation, and function. Exp Cell Res 2006;312(5):584–93.
[7] Bagri A, Tessier-Lavigne M, Watts RJ. Neuropilins in tumor biology. Clin Cancer Res 2009;15(6):1860–4.
[8] Pan Q, Chanthery Y, Liang WC, Stawicki S, Mak J, Rathore N, et al. Blocking neuropilin-1 function has an additive effect with anti-VEGF to inhibit tumor growth. Cancer Cell 2007;11(1):53–67.
[9] Berge M, Allanic D, Bonnin P, de Montrion C, Richard J, Suc M, et al. Neuropilin-1 is upregulated in hepatocellular carcinoma and contributes to tumour growth and vascular remodelling. J Hepatol 2011;55(4):866–75.
[10] Cao S, Yaqoob U, Das A, Shergill U, Jagavelu K, Huebert RC, et al. Neuropilin-1 promotes cirrhosis of the rodent and human liver by enhancing PDGF/TGF-beta signaling in hepatic stellate cells. J Clin Invest 2010;120(7):2379–94.
[11] Wang L, Zhao X, Feng Y, Ma X, Wu H, Zhu Q. Intrahepatic angiogenesis increases portal hypertension in hepatitis B patients with cirrhosis. Hepatol Res 2017;47(3):E94-103.
[12] Coulon S, Heindryckx F, Geerts A, Van Steenkiste C, Colle I, Van Vlierberghe H. Angiogenesis in chronic liver disease and its complications. Liver Int 2011;31(2):146–62.
[13] Herzog B, Pellet-Many C, Britton G, Hartzoulakis B, Zachary IC. VEGF binding to NRP1 is essential for VEGF stimulation of endothelial cell migration, complex formation between NRP1 and VEGFR2, and signaling via FAK Tyr407 phosphorylation. Mol Biol Cell 2011;22(15):2766–76.
[14] Fantin A, Herzog B, Mahmoud M, Yamaji M, Plein A, Denti L, et al. Neuropilin 1 (NRP1) hypomorphism combined with defective VEGF-A binding reveals novel roles for NRP1 in developmental and pathological angiogenesis. Development 2014;141(3):556–62.
[15] Gelfand MV, Hagan N, Tata A, Oh WJ, Lacoste B, Kang KT, et al. Neuropilin-1 functions as a VEGFR2 co-receptor to guide developmental angiogenesis independent of ligand binding. Elife 2014;3:e03720.
[16] Murga M, Fernandez-Capetillo O, Tosato G. Neuropilin-1 regulates attachment in human endothelial cells independently of vascular endothelial growth factor receptor-2. Blood 2005;105(5):1992–9.
[17] Koch S, Claesson-Welsh L. Signal transduction by vascular endothelial growth factor receptors. Cold Spring Harb Perspect Med 2012;2(7):a006502.
[18] Kofler NM, Simons M. Angiogenesis versus arteriogenesis: neuropilin 1 modulation of VEGF signaling. F1000Prime Rep 2015;7:26.
[19] Ohie S, Udagawa Y, Aoki D, Nozawa S. Histoculture drug response assay to monitor chemoresponse. Methods Mol Med 2005;110:79–86.
[20] Sun S, Wu HJ, Guan JL. Nuclear FAK and its kinase activity regulate VEGFR2 transcription in angiogenesis of adult mice. Sci Rep 2018;8(1):2550.
[21] Taura K, De Minicis S, Seki E, Hatano E, Iwaisako K, Osterreicher CH, et al. Hepatic stellate cells secrete angiopoietin 1 that induces angiogenesis in liver fibrosis. Gastroenterology 2008;135(5):1729–38.

[22] Sakata K, Eda S, Lee ES, Hara M, Imoto M, Kojima S. Neovessel formation promotes liver fibrosis via providing latent transforming growth factor-β. Biochem Biophys Res Commun 2014;443(3):950–6.

[23] Liu L, You Z, Yu H, Zhou L, Zhao H, Yan X, et al. Mechanotransduction-modulated fibrotic microniches reveal the contribution of angiogenesis in liver fibrosis. Nat Mater 2017;16(12):1252–61.

[24] Glinka Y, Prud'homme GJ. Neuropilin-1 is a receptor for transforming growth factor beta-1, activates its latent form, and promotes regulatory T cell activity. J Leukoc Biol 2008;84(1):302–10.

[25] Ballmer-Hofer K, Andersson AE, Ratcliffe LE, Berger P. Neuropilin-1 promotes VEGFR-2 trafficking through Rab11 vesicles thereby specifying signal output. Blood 2011;118(3):816–26.

[26] Shintani Y, Takashima S, Asano Y, Kato H, Liao Y, Yamazaki S, et al. Glycosaminoglycan modification of neuropilin-1 modulates VEGFR2 signaling. EMBO J 2006;25(13): 3045–55.

[27] Hamerlik P, Lathia JD, Rasmussen R, Wu Q, Bartkova J, Lee M, et al. Autocrine VEGF-VEGFR2-Neuropilin-1 signaling promotes glioma stem-like cell viability and tumor growth. J Exp Med 2012;209(3):507–20.

[28] Ren B, Deng Y, Mukhopadhyay A, Lanahan AA, Zhuang ZW, Moodie KL, et al. ERK1/2-Akt1 crosstalk regulates arteriogenesis in mice and zebrafish. J Clin Invest 2010;120 (4):1217–28.

[29] Gerber HP, McMurtrey A, Kowalski J, Yan M, Keyt BA, Dixit V, et al. Vascular endothelial growth factor regulates endothelial cell survival through the phosphatidylinositol 3′-kinase/Akt signal transduction pathway. Requirement for Flk-1/KDR activation. J Biol Chem 1998;273(46):30336–43.

[30] Kalluri R, Zeisberg M. Fibroblasts in cancer. Nat Rev Cancer 2006;6(5):392–401.